

Erbium doping influences morphological, structural and optical behavior of magnetite nanopowders

Richa Jain¹, Shubha Gokhale¹

^{1 & 2} School of Sciences, Indira Gandhi National Open University, Maidan Garhi, New Delhi, India
Email - richaj80@gmail.com

Abstract: In the present investigation, magnetite nanoparticles having formula $Fe_{3-x}Er_xO_4$ (where $x = 0$ to 0.05) have been synthesized using a convenient low temperature co-precipitation route. The change in structural, phase and optical properties has been studied as a function of doping level. The samples have been characterized using TEM, EDX SEM, XRD and UV-Vis spectroscopy. TEM images show the formation of rod like structures with erbium doping. X-Ray diffraction (XRD) patterns have been used to calculate the strain. Crystallite size is found to increase with erbium doping till a doping concentration of $x=0.01$. UV-Vis spectroscopy study shows the more absorbance peaks appear in the region of 600-850 nm with erbium doping which have been attributed to the f-f transitions in Erbium. Band-gaps are calculated using UV-Vis spectroscopy by Tauc plots. An increase in band-gap is found with erbium doping. Band-gap for undoped particle is 2.43 eV which decreases to 2.36 with erbium doping of $x=0.01$. Hence this technique can be used in band-gap tailoring.

Key Words: Magnetite, Erbium, Doping, UV-Visible study, Nanorods.

1. INTRODUCTION:

Magnetite (Fe_3O_4) nanoparticles are widely used functional materials due to excellent physical and chemical properties directed towards many applications. These have physical properties such as large surface area, good suspension stability and strong adsorption ability, thereby imparting specific magnetic, electrical and optical properties well suited for chemical, mechanical, electronic communications, biomedical, environmental protection and military applications. [1-2] The unique f-electron configuration of rare elements offers the shielding of 4f electrons by 5d and 6s electrons from environmental impact. It has been observed that rare earth doping in ferrites, enhances the structural, magnetic and optical properties. [3-5] Fe_3O_4 possesses inverse spinel structure and the substitution of other element ion in place of Fe^{3+}/Fe^{2+} ion can result into modified magnetic behavior. Erbium doping in cobalt and Ni-Zn ferrites improves the magnetic and transport properties. [6-8]

In the present investigation, the $Fe_{3-x}Er_xO_4$ (where $x = 0$ to 0.05) nanoparticles have been synthesized using the co-precipitation route. The change in structural, phase and optical properties has been studied as a function of doping level. The samples have been characterized using TEM, EDX SEM, XRD, and UV-Vis spectroscopy. TEM images show the formation of rod like structures with erbium doping whereas undoped particles are round shaped. X-Ray diffraction (XRD) patterns have been used to calculate the strain and crystallite size. Band-gaps are calculated using UV-Vis spectroscopy by Tauc plots. An increase in band-gap is found with erbium doping. Band-gap for undoped particle is 2.43 eV which decreases to 2.36 for erbium doping of $x=0.01$. Hence this technique can be used in band-gap tailoring.

2. EXPERIMENTAL DETAILS:

2.1. Synthesis

$Fe_{3-x}RE_xO_4$ (where x stands for 0 to 0.10 in steps of 0.01) particles were synthesized using an inexpensive co-precipitation method. Stoichiometric amounts of $FeCl_3$ and $ErCl_3$ were dissolved in de-ionized water to form 0.2 M solution. NaOH solution was added in this mixture to maintain the pH value of 10. This solution [solution- 1] was magnetically stirred at $80^\circ C$ for 2.5 hours. Stoichiometric amount of 0.2 M $FeSO_4$ and NaOH [solution-2] were ultrasonicated at room temperature for 5 min. Solution-2 was added to solution-1 at room temperature and ultrasonicated for 35 min. The product in the form of black precipitate was washed thoroughly in deionized water and finally with ethanol. Then the sample was vacuum dried to obtain the nanoparticles in the form of black powder.

2.2. Characterization

The TEM was used for studying the morphology of the nanoparticles. Samples for TEM were prepared by depositing a layer of ultra-dilute dispersion of nanoparticles in ethanol on the polymer coated copper grid and drying in air. TEM analysis was carried out using the JEOL 2100F operated at 200 keV electron energy. Field emission scanning microscopy / energy dispersive X-ray analysis (FESEM/EDX) was performed using Zeiss EVO40 Scanning Electron Microscope (SEM).

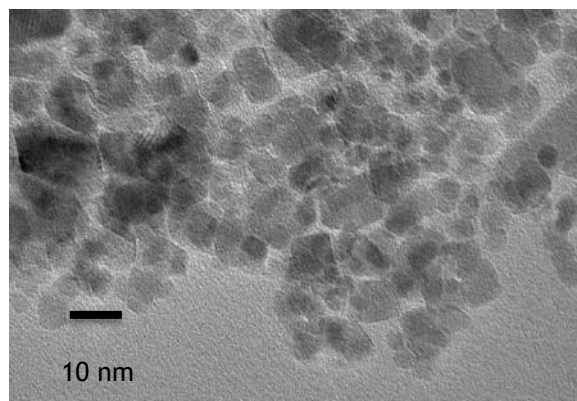
X-ray diffraction was carried out from 25° to 80° at room temperature using PANalytical X'pert PRO diffractometer with copper $K\alpha$ ($\lambda = 1.54\text{\AA}$) radiation.

The optical properties were determined at room temperature between a wavelength of 280 nm to 800 nm by using Systronics make UV-Vis spectrometer.

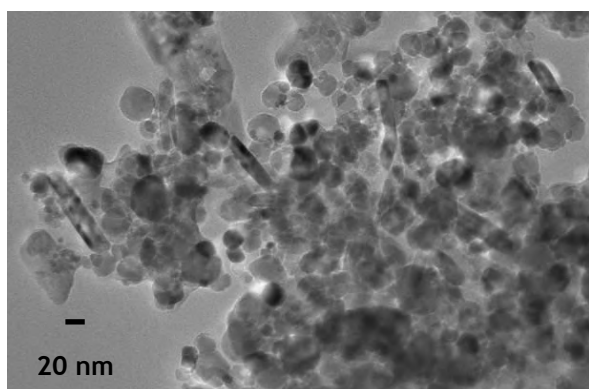
3. RESULTS AND DISCUSSIONS:

3.1. Morphological studies

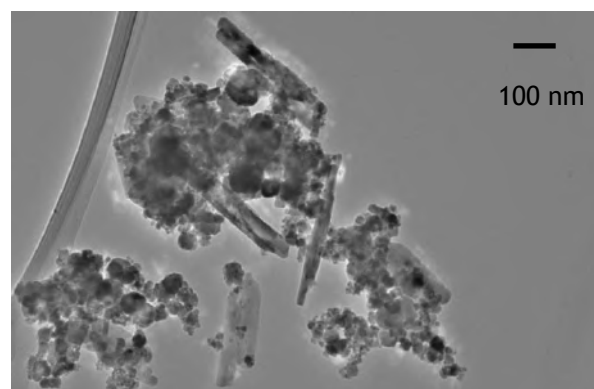
The transmission electron micrographs of $\text{Fe}_{3-x}\text{Er}_x\text{O}_4$ (for $x=0.0, 0.01$ and 0.03) are shown in Fig. 1(a, b, c). The micrographs obtained for doped samples show formation of rod-like structure. Undoped magnetite nanoparticles are the spherical particles. The TEM micrographs are shown in Fig.1.



(a)



(b)



(c)

Fig.2: TEM micrographs of $\text{Fe}_{3-x}\text{Er}_x\text{O}_4$ with $x =$ (a) 0.00; (b) 0.01 and (d) 0.03

The rods have nominal thickness (diameter) of 15 to 35 nm but their length increases significantly from 120 nm to 350 nm with doping. The aspect ratio is ~ 5 for $x = 0.01$ while it is ~ 10 for $x = 0.03$.

Sr. No.	Doping Concentration (x)	Rod Diameter (nm)	Rod Length (nm)	Aspect Ratio	Number of Rods (in $500\text{ nm} \times 500\text{ nm}$ area)
1	0	No rods	No rods	-	0
2	0.01	25-30	120-150	5	5
3	0.03	25-35	200-350	10	10

Table -1.

Strain produced in the lattice due to the insertion of erbium ions may lead to the formation of rod like structures. To check any stoichiometric variation in the sample, field emission scanning microscopy / energy dispersive X-ray analysis (FESEM/EDX) was performed for $x = 0.01$ sample.

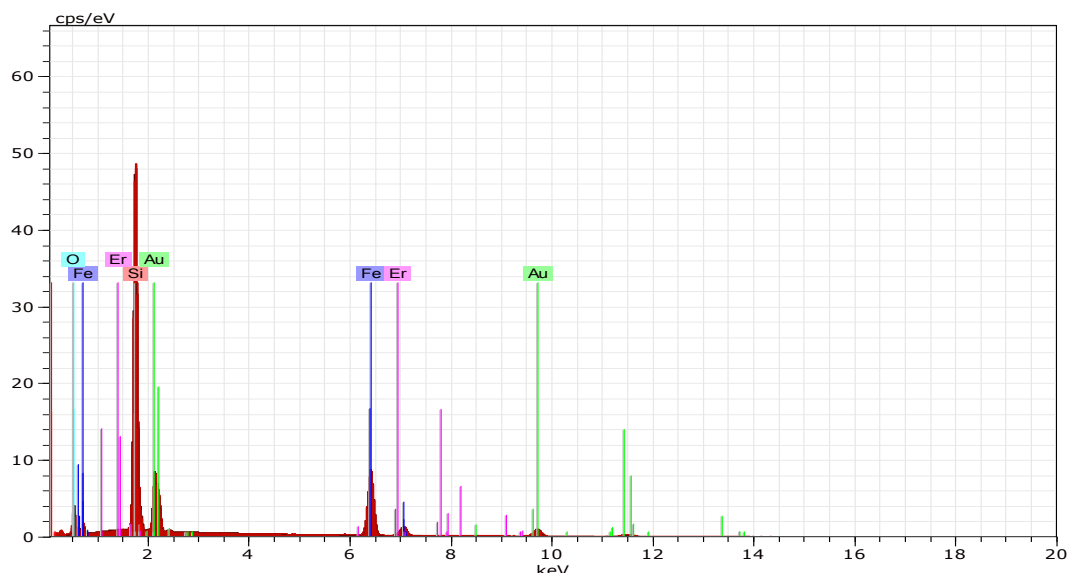


Fig.2: EDX spectrum of $\text{Fe}_{3-x}\text{Er}_x\text{O}_4$ with $x = 0.01$.

Element	Series	unn.	C norm.	C Atom.	C Error
Silicon	K-Series	41.62	30.94	51.17	1.8
Gold	M-Series	24.56	18.26	4.31	0.9
Iron	K-Series	61.66	45.84	38.12	1.8
Erbium	L-Series	4.11	3.05	0.85	0.1
Oxygen	K-Series	2.57	1.91	5.55	0.3
Total		134.51	100	100	0.3

Table. 2 Elemental composition of EDX spectrum.

Table .2 shows the elemental composition of samples. Hence EDX shows the presence of erbium in the prepared samples. SEM samples were prepared on silicon wafer and gold coating was done to prevent charging of the specimen.

3.2. XRD

X-ray diffraction (XRD) is a powerful nondestructive technique for characterizing crystalline materials. It provides information on crystal structure, phase, preferred crystal orientation (texture), and other structural parameters, such as average grain size, crystallinity,

XRD of magnetic nanoparticles of $\text{Fe}_{3-x}\text{Er}_x\text{O}_4$ (with $x=0.00, 0.01, 0.02, 0.03$ and 0.05) revealed that that prepared nanoparticles have good crystallinity and have face centred cubic spinel structure. This agrees with the XRD pattern of Fe_3O_4 (JCPDS card number 85-1436). XRD is shown in Fig.3. It is observed that with doping peaks attributed to the formation of ErFeO_3 (ASTM card number 74-1480).

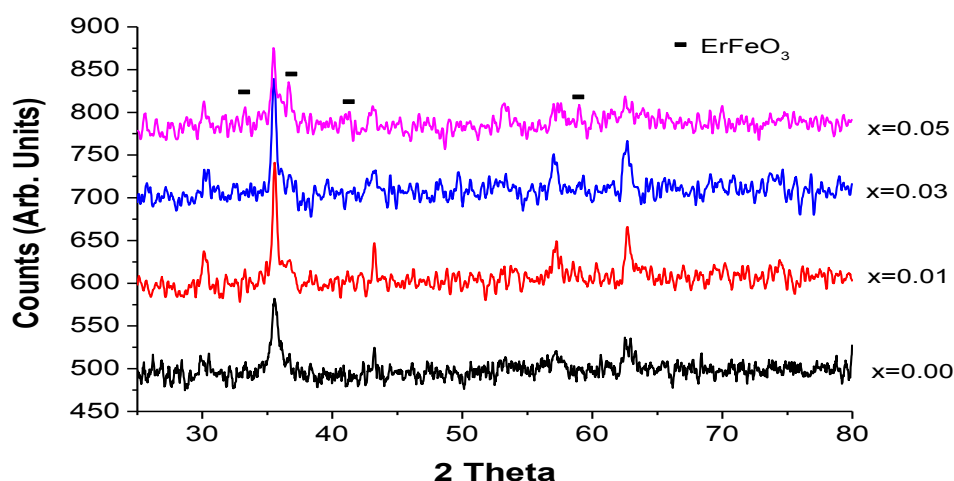


Fig 3: XRD of $\text{Fe}_{3-x}\text{Er}_x\text{O}_4$ (with $x=0.00, 0.01, 0.03$ and 0.05).

ErFeO₃ peaks become intense with increase in doping concentration. It has been reported that the dopant ions get incorporated by substitution of Fe³⁺ by Er³⁺ at octahedral site in the spinel structure of Fe₃O₄ to a limited extent. Larger amount of dopant results erbium ferrite phase. [3,5]

Crystallite size was calculated from the XRD data by using Scherrer formula for (311) peak at 35.57°:

$$\text{Crystallite size} = \frac{0.9\lambda}{\beta \cos\theta}$$

where β is the full width at half maximum, θ is the angle of diffraction and λ is the wavelength of X-ray ($\lambda = 1.54\text{\AA}$). Variation of crystallite size with doping is plotted in Fig. 4. The calculated crystallite size gradually increases from 13.9 nm for no doping to 24.1 nm for $x=0.01$ and then it reduces till 19.8 nm for $x=0.05$.

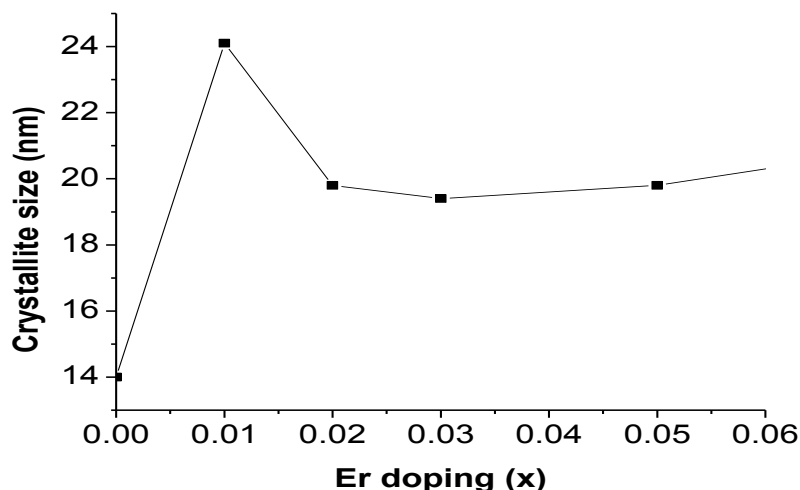


Fig 4: Plot of crystallite size verses doping of Fe_{3-x}Er_xO₄

The radius of erbium ions (0.088 nm) is about 1.4 times the radius of Fe³⁺ ion (ionic radius 0.064 nm) therefore during co-precipitation process some of the dopant ions would accumulate on the grain boundaries to form ultra-thin layer around the grains which may results in the formation of secondary phase after the doping. It has been observed that the diffraction pattern of erbium doped samples show a slight left shift in 2θ values relative to undoped samples These shifts in peak position give indication of incorporation of erbium in the spinel lattice. This could produce a mechanical stress in the crystal lattice due to incorporation of large radii erbium ions in magnetite nanopowders. [9]

The diffraction pattern showing the comparison of (311) peak which is main peak of the magnetite at about 35.7° for various Er³⁺ doping levels are presented in Fig.5. The strain in the structure has been found using the relation:

$$\varepsilon_s = -\Delta\theta_{(311)} \cot\theta_{(311)}$$

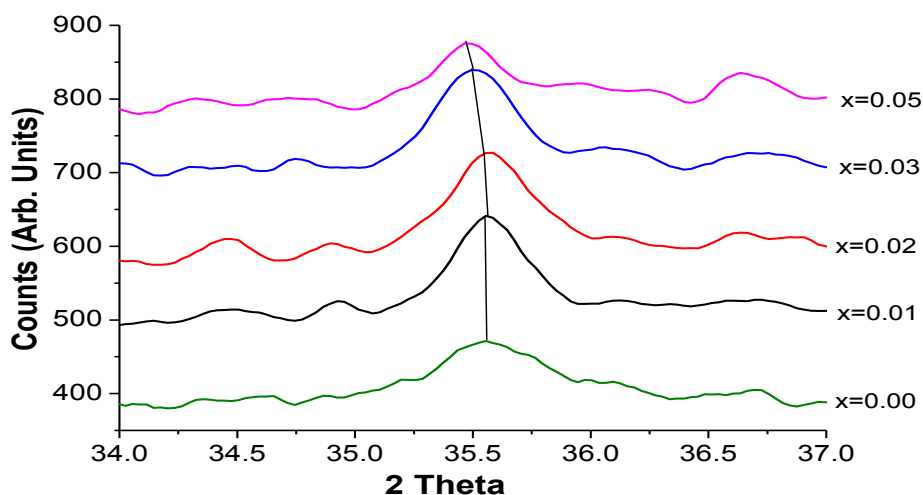


Fig.5: X-ray diffraction peak observed for (311) peak of Fe_{3-x}Er_xO₄ (with $x=0.00, 0.01, 0.03$ and 0.05)

Sample(x)	2 θ (deg)	$\Delta\theta$ (deg)	Cot θ	$\varepsilon_s(\text{radians}) \times 10^{-4}$
0	35.558	-	-	-
0.01	35.555	0.002	3.118	1.087
0.02	35.551	0.004	3.119	2.176
0.03	35.498	0.03	3.124	16.349
0.05	35.479	0.040	3.126	21.813

Table. 3 Strain calculation of Fe_{3-x}Er_xO₄ nanoparticles

The calculated values of strain are given in Table.3. Strain increases with erbium doping.

3.3. UV-Visible spectroscopy

Undoped sample has a peak near 3800 angstrom which is characteristic of magnetite [10] It is found to be slightly shifted towards the higher wavelength with erbium doping. With doping more absorbance peaks appear in the region of 6000-8500 angstrom, which have been attributed to the f-f transitions in Erbium [11]. A slight red shift in these peaks is observed with Er³⁺ doping as shown in Fig. 6.

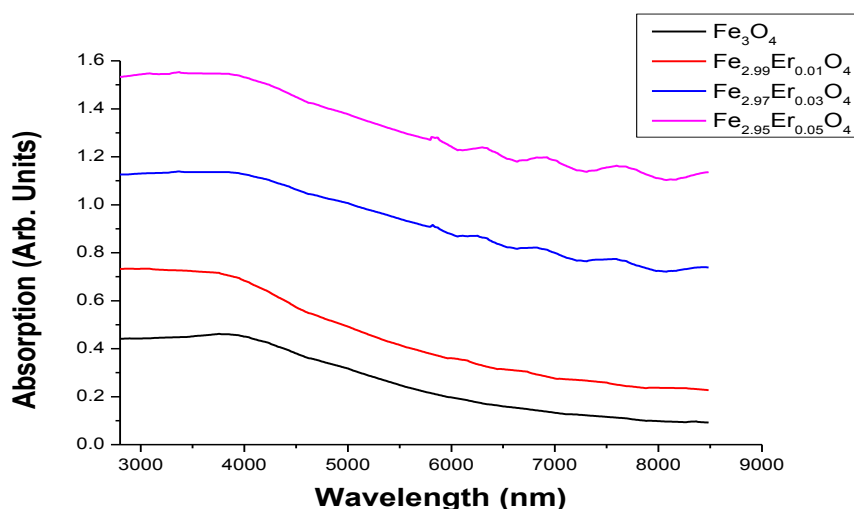


Fig.6: UV-Visible spectra of Fe_{3-x}Er_xO₄ (with x=0.00, 0.01, 0.03 and 0.05)

Band gap, which is also called energy gap, is the energy range between the conduction band and the valence band. The band gap is called "direct" if the momentum of electrons and holes is the same in both the conduction band and the valence band; an electron can directly emit a photon. The direct band gap of the nanoparticles is related to the optical gap (E_g) and photon energy ($h\nu$) according to the equation [12]

$$[\alpha h\nu]^2 = C(h\nu - E_g) \quad (1)$$

Where C is a constant, $n = 2$ for direct allowed transitions and α is the linear absorption coefficient.

The linear absorption coefficients, as a function of the photon energy were calculated as $\alpha(h\nu) = a(h\nu) \ln(10)/L$, where $a(h\nu)$ is the absorbance measured by using the UV-vis spectrophotometry, and L is the thickness of the sample cell. According to Eq. (1) The $[ah\nu]^n$ were plotted with $h\nu$. The band-gap can be determined by extrapolating the linear region of the curve represented to $ah\nu = 0$. These plots are called Tauc plots. Tauc plots for the undoped sample are shown in Fig. 7.

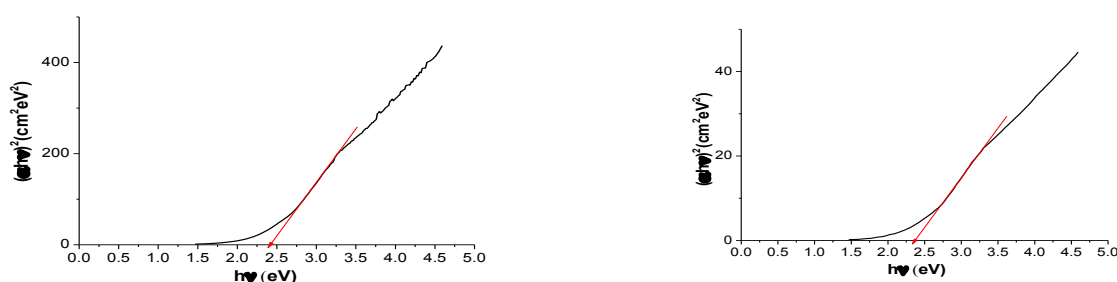


Fig. 7 Tauc plots for direct band-gap for (a) undoped (b) Er (0.01) doped samples.

The direct band-gap for undoped samples is 2.42 eV. Band-gaps vary with doping as shown Fig. 8 . The direct band-gap for Er doped (0.01) samples is 2.36 eV.

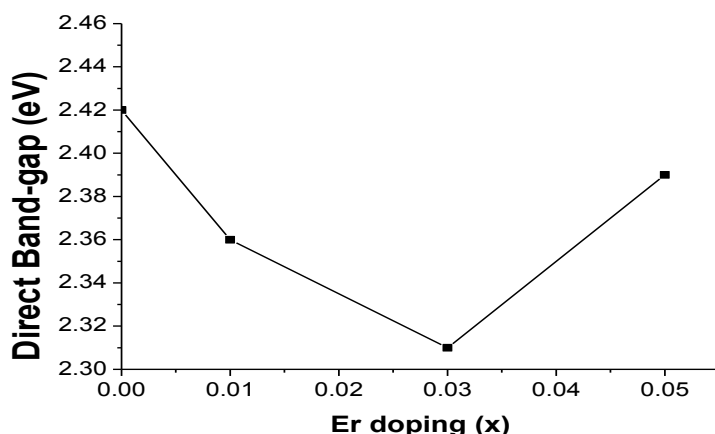


Fig.8: Variation of band gap of $\text{Fe}_{3-x}\text{Er}_x\text{O}_4$ (with $x=0.00, 0.01, 0.03$ and 0.05)

These bands - gaps are similar as the band-gap of semiconductors thus shows the semiconducting nature of our samples. The optical bandgap for visible light is 1-3 e V. The bandgap of synthesized nanoparticles falls in this range. The samples can be explored in photo sensing applications.

4. CONCLUSION

It has been observed that there is an improvement in the structural and optical properties of erbium doped magnetite. XRD results showed a strain is produced in the lattice with erbium doping. TEM micrographs showed the formation of rod like structure with erbium doping and density of rods increases with doping. UV-Visible study showed a slight red shift in these peaks with Er^{3+} doping. The direct band-gap for samples decreases with erbium doping.

5. ACKNOWLEDGMENT:

The TEM, XRD and EDX characterization was carried out at the Advanced Instrumentation Research Facility, Jawaharlal Nehru University, New Delhi. The UV-Vis characterization was carried out at IGNOU, New Delhi.

REFERENCES:

1. Tahereh B. Gorji and A.A. Ranjbar, A numerical and experimental investigation on the performance of a low-flux direct absorption solar collector (DASC) using graphite, magnetite and silver nanofluids, *Solar Energy* 135: 493-505, 2016.
2. N. Pramanik, T. RATH, R. Basu, J. de and P. P. Kundu, Fabrication of magnetite nanoparticles doped reduced graphene oxide grafted polyhydroxyalkanoate nanocomposite for tissue engineering application, *RSC Adv* 6.52: 46116-46133, 2016.
3. R. Jain, V. Luthra and S. Gokhale, Dysprosium doping induced shape and magnetic anisotropy of $\text{Fe}_{3-x}\text{Dy}_x\text{O}_4$ ($x=0.01-0.1$) nanoparticles, *J. Magn. Mater.* 414 :111-115, 2016.
4. H. Zhang, V. Malik, S. Mallapragada and M. Akinc, Synthesis and characterization of Gd-doped magnetite nanoparticles, *J. Magn. Mater.* 423: 386-394, 2017.
5. S. Prathapani, T. V. Jayaraman, E. K. Varaprasadarao, and D. Das, Effect of Er doping on the structural and magnetic properties of cobalt-ferrite, *Journal of Applied Physics* 116: 17A502-1-3, 2014.
6. Imran Ahmad, Tahir Abbas, A.B. Ziya, Asghari Maqsood, Structural and magnetic properties of erbium doped nanocrystalline Li-Ni ferrites *Ceramics International* 40 : 7941-7945, 2014.
7. Myrtil L. Kahn and Z. John Zhang, Synthesis and magnetic properties of spinel ferrite nanoparticles doped with lanthanide ions, *Appl. Phys. Lett.* 78: 3651-3653, 2001.
8. Widanarto, W., Sahar, M.R., Ghoshal, S.K., Arifin, R., Rohani, M.S. and Hamzah, K, Effect of natural Fe_3O_4 nanoparticles on structural and optical properties of Er^{3+} doped tellurite glass, *J. Magn. Mater.* 326: 123-128, 2013.
9. Xiruo Zhao, Wei Wang, Yajun Zhang, Sizhu Wu, Feng Li and J. Ping Liu, Synthesis and Characterization of gadolinium doped cobalt ferrite nanoparticles with enhanced adsorption..., *Chemical Engineering Journal*, 250:164-174, 2014.
10. Sachin A. Kulkarni, P.S. Sawadh, Prakash K. Palei and Kiran K. Kokate. Effect of synthesis route on the structural, optical and magnetic properties of Fe_3O_4 nanoparticles, *Ceramics International*, 40(2014)1945-1949.
11. YUAN Haibin, ZHANG Jianhui, YU Ruijin and SU Qiang, Synthesis of rare earth sulfides and their UV-vis absorption spectra, *Journal of rare earth* 27: 308-311, 2009.
12. D. Espinosa, L. B. Carlsson, and A. M. Figueiredo Neto, Influence of nanoparticle size on the nonlinear optical properties of magnetite ferrofluids, *Physical Review E* 88: 0323021-7, 2013.